2-22-2016

Ultrafast imaging of isolated molecules with electron diffraction

Martin Centurion
University of Nebraska-Lincoln, martin.centurion@unl.edu

Published in *Journal of Physics B: Atomic, Molecular and Optical Physics* 49 (2016), 062002 (15pp).
doi 10.1088/0953-4075/49/6/062002

Submitted 2 December 2014; revised 9 December 2015; accepted 3 January 2016; published 22 February 2016.

Topical Review

Ultrafast imaging of isolated molecules with electron diffraction

Martin Centurion

University of Nebraska–Lincoln, USA
email martin.centurion@unl.edu

Abstract

Recent advances in ultrafast electron diffraction offer the possibility to image isolated molecules with sub-Angstrom spatial resolution in ultrafast time scales. In particular, diffraction from aligned molecules has opened the door to retrieving three-dimensional structures directly from experimental data. In this manuscript we review the progress in ultrafast gas electron diffraction and discuss remaining challenges to achieve a temporal resolution of sub-100 fs, which is needed to observe the nuclear motion in chemical reactions in the gas phase.

Keywords: ultrafast electron diffraction, molecular imaging, ultrafast imaging, gas electron diffraction, femtosecond electron diffraction, molecular structure

1. Introduction

Imaging changes in molecular structure as they take place is important for understanding, and ultimately controlling, chemical reactions. Investigating isolated molecules is of particular interest to understand how light is converted to chemical energy and heat at the molecular level through structural rearrangement of the nuclei. The advent of femtosecond lasers has enabled researchers to investigate photoinduced reactions on the primary time scale on which they take place [1–4]. Most of the known information has been obtained through spectroscopic experiments that provide information on the energy landscape of the molecule and how it evolves with time [5–11]. Ultrafast diffraction experiments are sensitive to the molecular structure, and thus provide spatial information that is complementary to the spectroscopic measurements. If the wavelength of the radiation used for diffraction (either x-rays or electrons) is shorter than an Angstrom, it is possible to retrieve molecular structures with atomic resolution. In comparison with x-rays, electron diffraction has the advantage of higher scattering cross sections [12]. The promise of ultrafast diffraction experiments in the gas phase is to map, in three-dimensions (3D), the position of all nuclei in a molecule as a reaction takes place. Reaching this goal, however, imposes very challenging conditions on the experiments and data analysis that have so far prevented making such a molecular movie of the dynamics of isolated molecules. Significant progress has been made in capturing atomically resolved reactions in condensed matter [13, 14].

There are two major challenges that need to be met for ultrafast electron diffraction (UED) in the gas phase to capture molecular dynamics. The first is to reach a sufficient temporal resolution (100 fs) to capture the motion of atoms in real time and in some cases as short as 10 fs to follow dissociative channels. In a time-resolved pump-probe experiment, the sample is excited (pumped) by a laser pulse, and probed by an electron pulse. This requires not only the ability to deliver sufficiently short electron pulses on target, but also to match the group velocity of the electrons to that of the laser pulse that excites the molecules.

The second challenge is to retrieve the molecular structure from the diffraction pattern. When diffracting from molecules in the gas phase, the random orientation of the molecules greatly reduces the information content of the diffraction patterns. In this case, the structure is not retrieved directly from the data, but by comparing the measured patterns to a theoretical model and optimizing the model to best fit the data [15]. Retrieving

the structure without the need of a theoretical model would make the method more powerful, particularly when measuring the structure of transient states. Diffraction patterns from aligned molecules contain enough information to retrieve the structure, provided the molecular structure is simple and the alignment is sufficiently narrow [16–19]. For larger structures, simulations have shown that sub-nanometer resolution can be achieved in diffracting from a virus that is aligned by a continuous laser beam [20].

This manuscript will review progress in electron diffraction from gas-phase molecules aligned with laser pulses. We will cover the progress from the first experiments that were able to detect alignment through electron diffraction [21–24], to more recent results where molecular structures were retrieved directly from the diffraction data [18, 25]. The method of laser-alignment inherently requires ultrafast temporal resolution, in particular when the molecules are impulsively aligned. In this case, the alignment is transient with a lifetime of only a few picoseconds. The rest of the manuscript is divided as follows: section 2 describes the method of static gas electron diffraction (GED). Section 3 discusses the temporal resolution and gas-phase UED experiments with picosecond resolution. Section 4 describes the method of ultrafast electron diffraction from aligned molecules, including theory and experimental results. In section 5 we will describe current limitations and recent advances, and close in section 6 with an outlook of the progress that we expect over the next few years.

2. Gas electron diffraction

The first GED experiment was reported in 1930 [26], and since then GED has become a standard technique for measuring static structures of isolated molecules [15]. The main advantage of GED is that it provides sub-Angstrom spatial resolution in very compact set-ups. A continuous beam of electrons with kinetic energy typically in the range of 10–100 keV is crossed with a molecular beam in a vacuum chamber. The scattering pattern is captured using a two-dimensional (2D) imaging detector such as a photographic plate or a phosphor screen that is imaged on a CCD camera. The interference of waves scattered from different atoms within individual molecules results in circular rings in the diffraction pattern. Due to the random orientation of the molecules the diffraction patterns contain only one-dimensional (1D) structural information, i.e. the distances between atom pairs. For molecules with more than a few atoms, the information is not sufficient to directly extract the structure from a diffraction pattern because many of the distances will overlap. The data is analyzed by comparing the measurement to a model of the structure, and refining the structure of the model to find the best fit to the experimental data. The optimization routine can also include the results of other experiments and quantum chemical simulations that provide constraints for the optimization [27–31]. This method has been successful in determining structures to high precision by applying strong constraints from theory in order to determine the structure.

In GED the diffraction pattern is composed of the incoherent sum of the scattering from individual molecules. The transverse coherence of the electron beam is smaller than the intermolecular distance in the gas, but larger than the size of the molecules. In order to calculate the diffraction from a single molecule, we assume a molecule at the origin of the coordinate system and an electron beam propagating along the z-axis. For a molecule with N atoms, the total scattering intensity as a function of the polar scattering angle q and the azimuthal angle f is given by

$$\begin{aligned} I_{\text{Total}}(\theta,\ \phi) &= \frac{I_0}{D^2(\theta)}\left|\sum_{n=1}^{N} f_n(\theta)\exp(\mathrm{i}\vec{s}\cdot\vec{r_n})\right|^2 \\ &= \frac{I_0}{D^2(\theta)}\sum_{i=1}^{N}\sum_{j=1}^{N} f_i(s) f_j^*(s) \\ &\quad\times\exp(\mathrm{i}\vec{s}\cdot\vec{r_{ij}}) \end{aligned} \tag{1}$$

where I_0 is a constant, $\vec{r_n}$ is the position of the nth atom, $\vec{r_{ij}} = \vec{r_i} - \vec{r_j}$ is the vector pointing from the ith to the jth atom, $\vec{s} = \vec{k} - \vec{k_0}$ is the wave vector change for diffracted electrons, $D(q)$ is the distance from the origin to the detector position with angular coordinate (q), $f_n(q)$ is the scattering amplitude of the nth atom, $k = 2\pi/\lambda$ is the wavenumber of the electrons, $\vec{k}$ and $\vec{k_0}$ are the average wave vectors for the scattered and incident electron beams, respectively, and l is the de Broglie wavelength. The waves scattered from each atom interfere at the detector, which records the intensity of the wave.

Most GED experiments to date have been performed with randomly oriented molecules. In this case the diffraction pattern can be calculated by averaging over all possible angular orientations of the molecule [15]. We introduce two angles (α, β) to represent the orientation of the molecules in the sample, where α is the polar angle and β is the azimuthal angle with respect to $\vec{s}$. The magnitude of the wave vector change is $s(\theta) = 2k\sin(\theta/2)$, using this relation we change the argument from θ to s and write for the scattering intensity with randomly oriented molecules:

$$\begin{aligned} I_{\text{Random}}(s) &= 1/4\pi\int_0^{2\pi}\int_0^{\pi}\frac{I_0}{D^2(s)}\sum_{i=1}^{N}\sum_{j=1}^{N} f_i(s) f_j^*(s) \\ &\quad\times\exp(\mathrm{i}sr_{ij}\cos\alpha)\sin\alpha\,\mathrm{d}\alpha\,\mathrm{d}\beta \\ &= \frac{I_0}{D^2(s)}\sum_{i=1}^{N}\sum_{j=1}^{N} f_i(s) f_j^*(s)\frac{\sin(r_{ij}s)}{r_{ij}s}. \end{aligned} \tag{2}$$

The double summation is over all atoms in the molecule. Notice that in this case there is no dependence on the azimuthal angle φ. Figure 1 shows, as an example, the diffraction intensity of the Diiodotetrafluoroethane molecule ($C_2F_4I_2$). Figure 1(a) shows a model of the molecule, and (b) shows the total scattering I_{Random}, which decreases rapidly with s.

The total scattering intensity can be split into an atomic and a molecular contribution. Assuming that the distance R from the molecules to the detector is much larger than the size of the detector, so that r is approximately constant over the flat surface

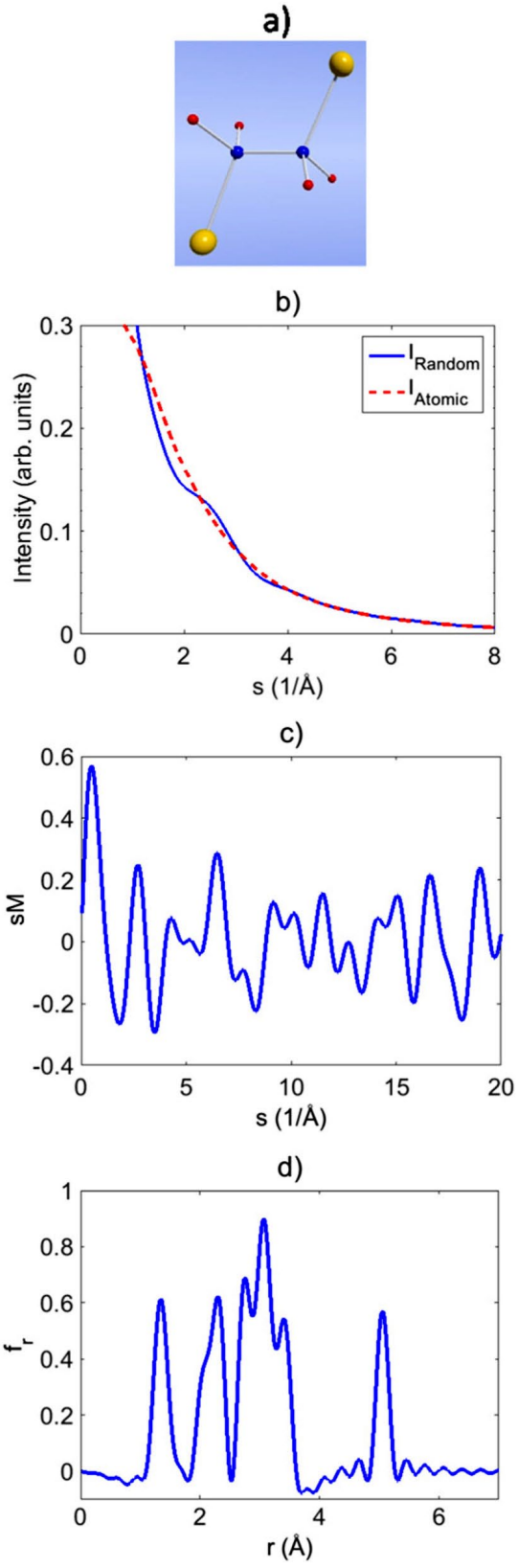

Figure 1. Gas electron diffraction of the $C_2F_4I_2$ molecule. (a) Model for the molecule. (b) Total scattering intensity I_{Random} (solid blue line) and atomic scattering intensity I_{Atomic} (dashed red line). (c) Modified scattering intensity sM. (d) Radial distribution function g_r. The calculations in parts (c) and (d) assume $s_{Max} = 20$ Å^{-1}.

of the detector, the total intensity can be expressed as:

$$I_{\text{Random}}(s) = I_{\text{Atomic}}(s) + I_{\text{Molecular}}(s) \tag{3a}$$

$$I_{\text{Atomic}}(s) = \frac{I_0}{R^2}\sum_{i=1}^{N}|f_i(s)|^2 \tag{3b}$$

$$I_{\text{Molecular}}(s) = \frac{I_0}{R^2}\sum_{\substack{i=1\\ i\neq j}}^{N}\sum_{j=1}^{N}|f_i(s)||f_j(s)| \times \cos[\eta_i(s) - \eta_j(s)]\frac{\sin(r_{ij}s)}{r_{ij}s} \tag{3c}$$

where $|f_i(s)|$ and η_i are the amplitude and phase of the form factor of the ith atom, respectively [32]. $I_{\text{Molecular}}$ contains the interference terms and thus the structural information, while I_{Atomic} depends only on the atomic scattering amplitudes and acts as a background that decreases rapidly with increasing scattering angle. After the angular averaging due to the random orientation, the structural information is still present but only as a weak modulation in the overall scattering intensity I_{Random}. Figure 1(b) shows both I_{Random} and I_{Atomic}. There is a modulation of I_{Random} around the values of I_{Atomic} that decreases in amplitude for larger scattering angles. The atomic scattering I_{Atomic} does not depend on the structure and can be calculated from the values of the form factor available in the literature.

The modified molecular scattering sM is created by rescaling $I_{\text{Molecular}}$ to bring up the interference fringes. The sM can be extracted from the measured I_{Random}:

$$sM = \frac{(I_{\text{Random}} - I_{\text{Atomic}})s}{I_{\text{Atomic}}} = \frac{s\, I_{\text{Molecular}}}{I_{\text{Atomic}}} = \frac{1}{\sum_{i=1}^{N}|f_i(s)|^2}\sum_{\substack{i=1\\ i\neq j}}^{N}\sum_{j=1}^{N}|f_i(s)||f_j(s)| \times \cos[\eta_i(s) - \eta_j(s)]\frac{\sin(r_{ij}s)}{r_{ij}} \tag{4}$$

As can be seen in figure 1(c), sM contains the interference pattern due to multiple atoms. Equation (4) shows that each interatomic distance corresponds to a sine function in sM. For diatomic molecules, sM will be sinusoidal. The radial distribution function $g_r(r)$, which picks out the interatomic distances r_{ij}, is calculated by taking a sine-transform of sM:

$$g_r(r) = \int_0^{s_{\text{Max}}} sM(s)\sin(rs)e^{(-\gamma s^2)}\mathrm{d}s \tag{5}$$

where s_{Max} is the maximum measured value of s, and γ is a damping constant that is adjusted to avoid edge effects in the transform. The function g_r has a peak corresponding to the distance between each atom pair in the molecule. Figure 1(d) shows g_r calculated from the sM in (c). The spatial resolution δ (the width of each peak) is determined by the wavelength of the electrons λ and by s_{Max}:

$$\delta = 2\pi/s_{\text{Max}} \tag{6}$$

For the example in figures 1(c) and (d), $\delta = 0.31$ Å. The interatomic distances are determined by finding the center of the peaks in g_r, and can therefore be determined to an accuracy significantly better than δ as long as there are no overlapping peaks. However, since GED projects all distances along one dimension, there are often multiple overlapping peaks and thus not enough information to retrieve the structure. Figure 1(d) shows clearly that there are fewer peaks than interatomic distances in the molecule.

The spatial resolution determines the smallest distance between two atoms where they can still be distinguished from each other, whilst the coherence length determines the largest object that can be measured. The coherence length is typically larger than the size of a single molecule, but smaller than the intermolecular distance in the gas sample. The transverse coherence of the beam can be modified by changing the size of the beam, at the cost of reduced density of electrons.

The formulas for the diffraction pattern can be simplified for the cases when the molecules are perfectly aligned and for the case where the orientation is random. For the case of partial alignment one must calculate the pattern due to a single molecule at different orientations with respect to the electron beam, and then average the patterns weighting their contributions according to the angular distribution. If the alignment is high, the patterns may contain enough information to retrieve the structure in 2D or in 3D, in which case peaks that overlap in a 1D projection can be separated [16–19]. In the case where the alignment is weak, the patterns could be used along with the random orientation patterns to provide additional data in the optimization routine.

3. UED from molecules in the gas phase

With the development of the femtosecond laser, it became possible to probe molecular dynamics in real time using spectroscopic measurements, which led to the field of femtochemistry [1–11]. Spectroscopic methods measure changes in the energy landscape of molecules as they undergo a reaction. Ultrafast diffraction experiments provide complementary information, i.e. the structure of the transient intermediate states in a reaction, which cannot be directly measured by other means. Using laser-triggered electron sources, it is now possible to generate femtosecond electron pulses. As a result, UED experiments in condensed matter have been used to observe a range of ultrafast processes with femtosecond resolution and are currently approaching the 100 fs level [13, 14, 33–35]. Performing diffraction experiments with molecules in the gas phase, however, brings additional challenges that have so far prevented experiments from reaching a comparable resolution.

3.1. Temporal resolution of gas-phase UED experiments

There are four contributions to the temporal resolution in a gas-phase UED experiment: (i) the duration of the laser pulse used to excite the sample, (ii) the duration of the electron pulse, (iii) the group velocity mismatch (GVM) between electron and laser pulses, and (iv) the time-of-arrival jitter between electron and the laser pulses, when radio-frequency (RF) acceleration or compression is used. The timing jitter introduced by RF fields is discussed in section 5.2. The GVM is due to the time it takes for the electron and laser pulses to traverse the sample, and depends on the speed of the electrons, the beam sizes and the relative angle between laser and electron beams [36]. The duration of the laser pulse is typically not a limiting factor, since sub-50 fs laser pulses have become standard. The duration of the electron pulses on target is determined by the duration of the laser pulse that triggers the emission, the initial energy spread of the electron pulse after photoemission, and the spreading during propagation due to Coulomb forces [37].

A high extraction field on the photocathode and a very short propagation distance minimizes the effects of the energy spread and space charge. In condensed matter systems UED has reached a resolution of less than 100 fs when considering time stamping and RF pulse compression [38], and similar resolution with the compact electron gun design [34, 35, 39] by reducing the distance from the photocathode to the target and limiting the number of electrons per pulse. The highest time resolution reported to date for any structural change is 180 fs for the electronically driven melting of bismuth [39]. The time stamping and compact guns used for condensed matter experiments, however, cannot be directly applied to gas-phase experiments. Gas phase diffraction does not produce diffraction spots to be streaked, although the transmitted beam could in principle be streaked. A high extraction field requires a high vacuum, which is incompatible with a gas source at a short distance from the photocathode. Furthermore, a short propagation distance does not solve the problem of GVM. So far, the shortest source to target distance that has been used in a gas-phase UED experiment has been 10 cm [18], which made it possible to deliver 25 keV pulses containing 2000 electrons with a duration of 500 fs on target. In this case, the resolution was limited by GVM.

The GVM can be understood based on geometrical factors and differences in velocity between the electron structural probe pulse and the laser excitation pulse. In laser pump–laser probe experiments, two collinear laser pulses traverse the sample with a fixed delay between them. For non-relativistic electrons, the time delay between the laser pump pulse and the electron probe pulse changes significantly as they traverse the sample. For example, the speed of an electron with a kinetic energy of 30 keV is 0.33 c, where c is the speed of light in vacuum. For a thin gas sample with a length of 200 μm, it takes 0.67 ps for the laser to traverse the sample, while it takes 2.0 ps for the electrons to traverse the same distance. Assuming the two pulses are collinear, the blurring of the temporal resolution from the GVM alone will be more than a picosecond. In the case where the laser and electrons are not collinear, the effect of GVM depends also on the angle and widths of the beams.

The total resolution of the experiment is given by

$$\Delta t = \sqrt{\tau_{\mathrm{GVM}}^2 + \tau_{\mathrm{e}}^2 + \tau_{\mathrm{L}}^2 + \tau_{\mathrm{J}}^2} \tag{7}$$

where τ_e and τ_L are the duration of the electron and laser pulses, respectively. τ_{GVM} is the GVM, τ_J is the time-of-arrival jitter between electron and laser pulses. In order to maximize the fraction of molecules that are excited and the fraction of electrons that are scattered it is optimal to match the size of all beams ($w = w_e = w_L = w_M$), where w_e, w_L and w_M are the widths of the electron, laser and molecular beams respectively. Experimentally it is more practical to have the laser and electron beams perpendicular to each other ($\theta = \pi/2$). Under these conditions the broadening due to GVD becomes [36]

$$\tau_{GVM} = \frac{w}{\sqrt{2}\,c}\sqrt{1 + A^2} \tag{8}$$

where $A = c/v_e$ is the ratio of the laser and electron speeds. For example, for $w = 100$ μm and $A = 3$, $\tau_{GVM} = 670$ fs. If $\tau_e = 500$ fs $\tau_L = 100$ fs and $\tau_J = 0$ (no RF fields), then the overall resolution $\Delta t = 840$ fs.

In the case where the electron speed approaches c, the collinear geometry ($\theta = 0$) becomes optimal. In this case the effect of GVM simplifies to:

$$\tau_{GVM} = \frac{w_M}{c}(A - 1) \tag{9}$$

For the collinear geometry the widths of the laser and electron beams do not play a role, while the width of the gas jet determines the propagation distance. Clearly, the effect of GVM vanishes as $A \to 1$.

While shorter electron pulses and less GVM can be achieved by increasing the kinetic energy of the electrons, for instance by raising the extraction field or increasing the acceleration length, in practice there is a tradeoff between the extraction field and the distance to the sample. The shortest distance is limited by the high vacuum required by the electron gun to sustain high electric fields without arching. An alternative approach to reduce the electron pulse duration is to use single-electron pulses to eliminate Coulomb broadening [40, 41]. Single-electron sources, however, are not practical for gas-phase UED due to the very low beam current. Alternative approaches to improve resolution are to use RF fields to compress the electron pulses [42, 43], using tilted laser pulses to compensate the GVM [44–46], and accelerating electrons to relativistic speeds [47–53]. These methods will be discussed further in section 5.2.

Figure 2 shows how the temporal resolution of gas-phase UED experiments has improved over the last 30 years. While many time-resolved experiments were performed over this time, the figure contains only a few representative results. In 1983, an experimental setup with a resolution of 1 μs was used to capture a diffraction pattern of the CF_3 radical after laser multiphoton photo-dissociation of the CF_3I molecule [54]. A decade later, the photolysis of 1,3-dichloroethenes with UV laser pulses was investigated with electron diffraction with a resolution of 15 ns [55]. Later on, the group of A. Zewail performed a series of experiments where the resolution was improved to the picosecond regime, demonstrating 15 ps resolution first [56], and soon after 5 ps [57] by using femtosecond lasers for photoemission and improving both the source and detectors in the experiment.

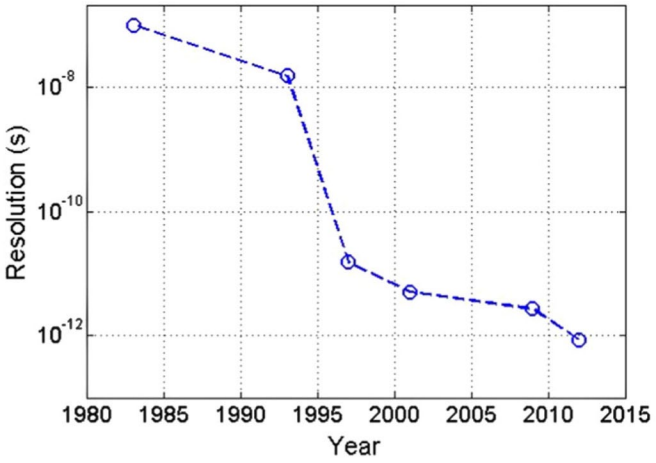

Figure 2. Temporal resolution in gas electron diffraction experiments. The data corresponds to the resolution demonstrated in a few representative experiments, corresponding to references [18, 23, 54– 57], respectively.

3.2. Transient molecular structures determined with picosecond resolution

The improvement to picosecond resolution was significant because it enabled structure determination of transient intermediate states [23, 24, 56–58]. Figure 3 shows the results of UED experiments on the photo-dissociation of the $C_2F_4I_2$ molecules carried out at Caltech in the Zewail group [57]. In this experiment, the molecules were excited by a UV femtosecond laser pulse that started a two-step reaction: $C_2F_4I_2 \to C_2F_4I + I \to C_2F_4 + 2I$, with time constants of approximately 200 fs and 30 ps, respectively. The time constants were measured previously with femtosecond laser time-of-flight mass spectrometry [59]. While the first step was too fast to capture with UED, the structure of the C_2F_4I transient was measured. The experiments were performed with both anti and gauche conformers present, as shown in the top panel of figure 3. Figure 3(b) shows the changes in the radial distribution function as a function of time, from which it was determined that, in the intermediate state, the iodine atom resides on one side of the molecule and is not shared by the two CF_2 moieties.

Further improvements in resolution were made by decreasing the distance from the source to the target and reducing the size of the gas, electron and laser beams resulting in an improvement in resolution to 3 ps [23]. Sub-ps resolution (850 fs) was achieved for the first time by shrinking the interaction volume of the laser, electron and gas beams to a diameter of 100 μm [18]. The improved resolution was crucial for the experiments with aligned molecules described in the following sections.

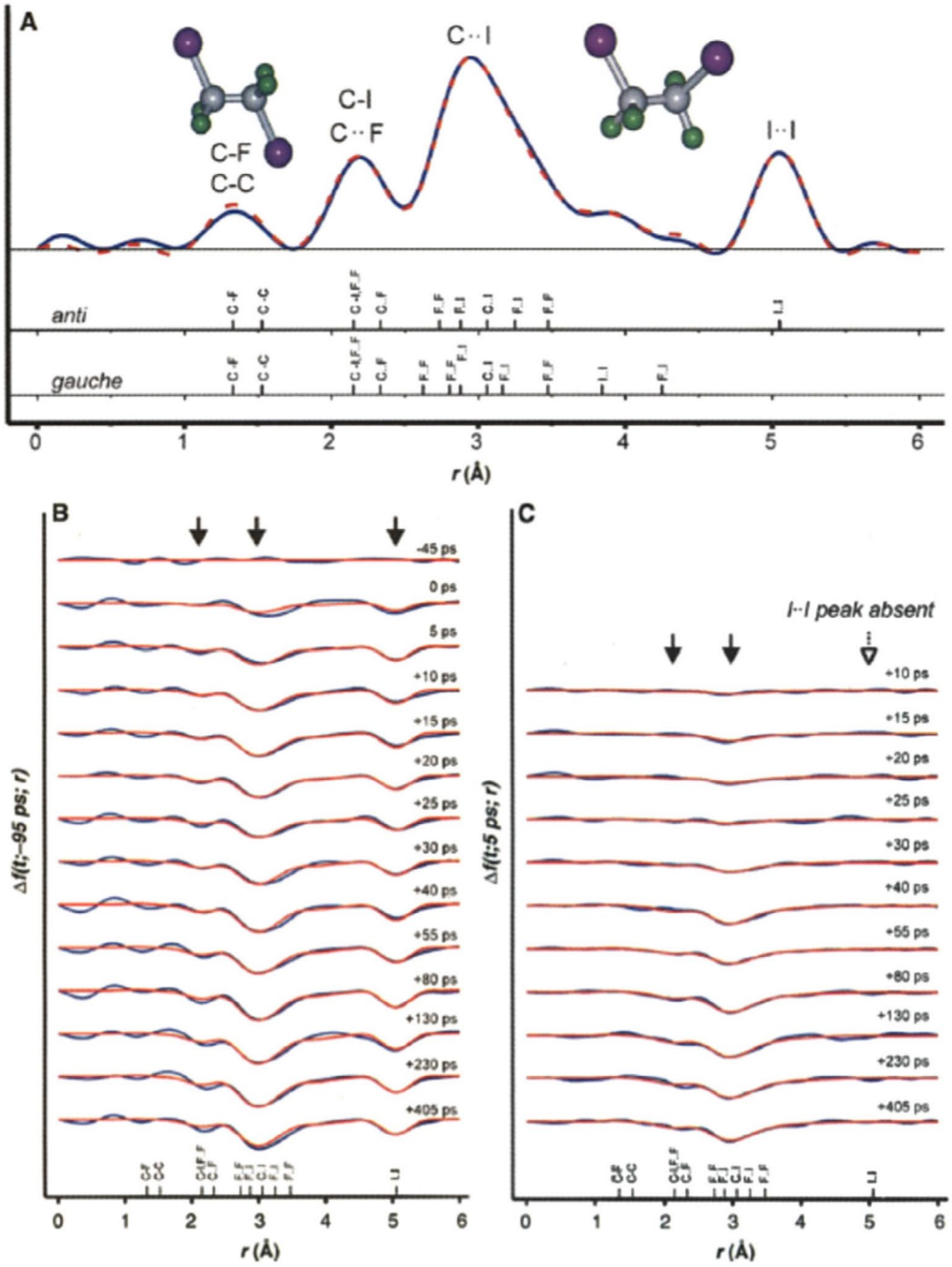

Figure 3. Time-resolved structural changes of $C_2F_4I_2$ during the elimination of iodine to form tetrafluoroethene. (**A**) Comparison of theoretical (red) and experimental (blue) radial distribution functions for the ground state of $C_2F_4I_2$; the interatomic distances for the anti and gauche structures are indicated for comparison. (**B** and **C**) Experimental curves referenced to −95 ps and to 5 ps, respectively (blue). Corresponding theoretical curves (red). Figure reproduced from [57].

4. Diffraction from aligned molecules

Diffraction methods can in principle reveal the full 3D structure of isolated molecules, but this is often prevented by the random orientation of molecules in the gas phase. As seen in figures 1 and 3, diffraction from randomly oriented molecules provides only 1D information. A Fourier analysis of the diffraction pattern results in the radial distribution function that contains peaks corresponding to the distances between pairs for atoms. Even for small molecules there is a large number of peaks at the short distance, for instance from 1 to 3Å (figures 1(c) and 3(a)). Larger molecules will also have many overlapping peaks at longer distances. The result is that the retrieved information is insufficient to uniquely determine the structure. Diffraction from aligned molecules can alleviate this limitation by projecting the structural information onto a two- or three-dimensional space, provided that the phase of the diffraction pattern can be retrieved. This requires the use of iterative retrieval algorithms and a high degree of alignment that increases as the molecules get larger [20]. For small molecules, it has been shown that

even with moderate alignment, the structure can be retrieved by combining multiple diffraction patterns [18, 19], although this method has not yet been tested on larger molecules. If the structure is successfully retrieved, peaks that overlap in 1D projections may be well separated when measured in 2D or 3D space.

4.1. Laser alignment of molecules

Intense laser light can be used to align non-polar molecules through an induced-dipole interaction. Laser alignment is a very active field to which many researchers have contributed [60]. Pulsed lasers are needed for alignment experiments in order to achieve high intensities. The duration of the laser pulses determines whether the alignment process is adiabatic or impulsive. When the pulse duration is longer than the rotational period of the molecule the alignment is adiabatic. In this case, the degree of alignment follows the intensity envelope of the laser pulse in time, i.e. alignment is highest when the laser intensity is maximal, and the ensemble returns to a random distribution when the laser intensity goes to zero. If the laser pulse duration is much shorter than the rotational period the alignment is impulsive. In the case of impulsive alignment with femtosecond laser pulses, a non-resonant pulse (with wavelength around 800 nm) creates a rotational wavepacket via Raman transitions. A higher laser intensity results in the excitation of higher rotational states and thus a narrower angular distribution. After an initial prompt alignment, the different rotational states in the wavepacket will dephase and the alignment disappears almost completely, although a small level of angular anisotropy remains. There are periodic revivals of the alignment at multiples of half the rotational period of the molecule.

For the purpose of determining molecular structures, it is preferable to capture a diffraction pattern of molecules in a field-free environment, free from the high intensity of the laser pulse that might distort the molecular structure or the diffraction process. This is particularly relevant for investigating transient states in photo-excited molecules which are likely to be affected by the presence of the alignment laser. The main advantage of impulsive alignment is that the molecules can be probed in this field-free environment, while the disadvantage is that the alignment is not as narrow as in the case of adiabatic alignment.

For the case of non-resonant impulsive alignment of a rigid linear molecule, the rotational state is described by two quantum numbers, $|J, M\rangle$, where J is the total angular momentum and M is the projection of J along the z-axis. For a linearly polarized laser pulse, under the rigid-rotor approximation, the Hamiltonian is given by:

$$H = \frac{B_e}{\hbar^2}\boldsymbol{J}^2 - \frac{1}{4}\varepsilon^2(t)\Delta\alpha\cos^2\chi \tag{10}$$

where B_e is the rotational constant of the molecule, $\varepsilon(t)$ is the laser electric field, $\Delta\alpha = \alpha_{\parallel} - \alpha_{\perp}$ is the anisotropy of the polarizability, $\alpha_{\parallel}$ and $\alpha_{\perp}$ are polarizability along the parallel and perpendicular direction with respect to the molecular axis of the linear molecule, and χ is the angle between molecular axis and laser polarization.

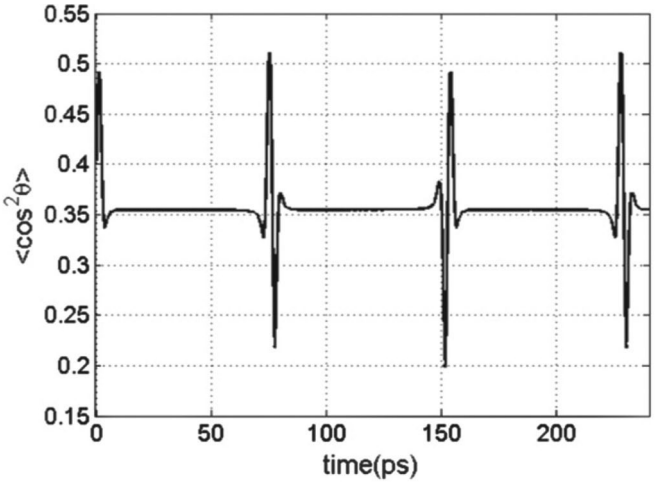

Figure 4. Simulation of impulsive laser alignment of CS_2. In this simulation the molecules had an initial rotational temperature of 30 K, and the laser pulse had a duration of 200 fs and fluence of 0.58 J cm^{-2}.

The laser excitation can be described using time-dependent Schrodinger's equation:

$$i\hbar\frac{\partial}{\partial t}\psi(t) = H(t)\psi(t) \tag{11}$$

For a thermal ensemble, the initial distribution of rotational states follows the Boltzmann distribution. Using equations (10) and (11), the laser excitation of impulsive alignment can be simulated numerically.

Figure 4 shows an example of the rotational dynamics following an impulsive excitation. The alignment of carbon disulfide (CS_2) was simulated by modeling the molecule as a linear rigid rotor that interacts with a non-resonant linearly polarized laser pulse described by the time-dependent Schrodinger equation [61, 62]. The angular distribution of the molecules is characterized by the parameter $\langle\cos^2\theta\rangle$, where the bracket denotes an ensemble average over all the molecules, and θ is the angle between the alignment axis (the direction of laser polarization) and the axis of each molecule. Random orientation results in a value of $\langle\cos^2\theta\rangle = 0.33$, while a value of $\langle\cos^2\theta\rangle = 1$ corresponds to perfect alignment. We have simulated a laser pulse duration of 200 fs, while the rotational period of the molecule is 152.8 ps. The alignment first peaks approximately 1 ps after the laser excitation, followed by periodic revivals at half the rotational period. Field free alignment is available at any of the alignment peaks.

4.2. Theory of diffraction from aligned molecules and structure retrieval

In the case of diffraction from aligned molecules, the diffraction patterns become anisotropic [63–67]. For a tutorial view on how alignment affects the diffraction patterns see [66]. If the angular distribution is known, the diffraction pattern can be calculated

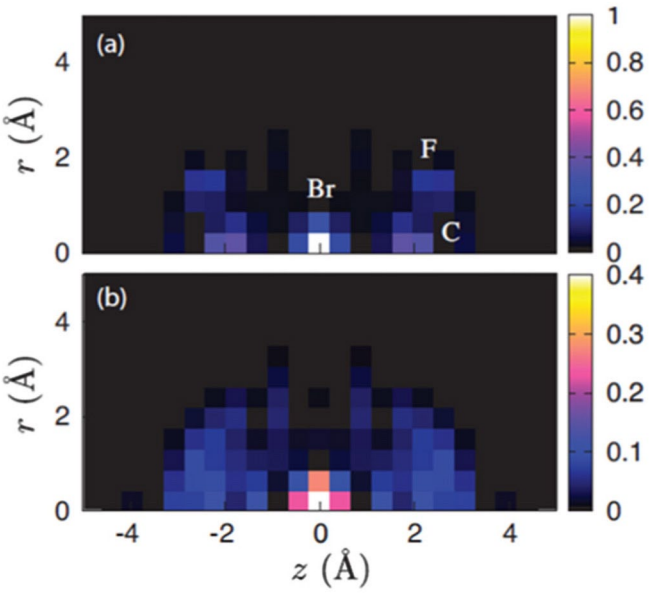

Figure 5. The azimuthally projected structure of CF_3Br, holographically reconstructed from simulated diffraction patterns. (**a**) Perfect 1D alignment and (**b**) laser-induced alignment. Figure reproduced from [17].

based on the diffraction pattern of a single molecule. The diffraction pattern is first calculated for a single molecule, then the molecule is rotated and a new diffraction pattern is calculated. Many such patterns are calculated to finely sample all angular orientations. Finally, the patterns are added incoherently, with weights given by the angular distribution. A more detailed description on how to calculate diffraction patterns from aligned molecules can be found in references [19, 65].

Interestingly, 1D alignment can be sufficient to retrieve 2D or even 3D information. In 1D alignment, only one axis of the molecule is fixed. If one molecular axis is fixed and the distribution of the other axes is random, the structure, when viewed as an average over many molecules, is cylindrically symmetric. It has been shown that in this case the structure can be retrieved using an iterative algorithm [16, 20]. In the special case where one of the atoms has a much higher scattering cross section than the others (has a higher atomic number Z), the structure can be retrieved directly with a holographic approximation using a Fourier–Hankel transform [17]. Theory shows that the diffraction pattern contains sufficient information to retrieve the structure, but the retrieval methods are not completely general and one needs to pick the one that will work best for a specific experimental situation. In addition, a very high degree of alignment is required for accurately retrieving the structure.

Figure 5 shows the retrieval of the structure of the trifluorobromomethane (CF_3Br) molecule using the holographic method [17]. CF_3Br is a symmetric top molecule with threefold symmetry. The simulated diffraction patterns were calculated up to a range of $s = 7\text{Å}^{-1}$, assuming 1D perfect and partial alignments. Figure 5(a) shows the retrieved structure of the case of perfect alignment, in cylindrical coordinates. In this case the structure of the molecule was retrieved accurately; note the position of the Br, C and F atoms (the three F atoms overlap in this 2D representation in cylindrical coordinates). This retrieval method relies on a Fourier–Hankel transform and therefore provides a 2D representation of the molecule in cylindrical coordinates r and z. Figure 5(b) shows the retrieval for the case of partial alignment with $\langle\cos^2\theta\rangle = 0.87$. Even though the alignment was very high, the structure is almost completely blurred out. The results show that accurate structures can in principle be retrieved from 1D perfectly aligned molecules, however, for a degree of alignment that can be achieved experimentally the structure could not be retrieved.

4.3. Observation of alignment with UED: adiabatic and selection through photoexcitation

The main experimental signature of alignment is that the measured diffraction patterns, unlike the case of random orientation, are not circularly symmetric. The anisotropy can be used to characterize the degree of alignment of the sample. The first measurement of anisotropic electron scattering was performed using a static electric field to orient methyl iodide (CH_3I) molecules [21]. The first detection of diffraction from laser-aligned molecules was performed by adiabatic alignment of carbon disulfide (CS_2) molecules with nanosecond laser pulses [22]. In this case the diffraction was measured using nanosecond electron pulses to capture a diffraction pattern while the molecules were aligned.

Alignment can also be achieved by selecting molecules lying along a particular direction. When a molecule is excited by a linearly polarized laser through a resonant process, the angular dependence of the excitation creates an anisotropic distribution of excited molecules. This can be used as a selection rather than actively imposing a torque on the molecules; the laser preferentially excites molecules with their dipole moment in a given direction. The first experimental demonstration of diffraction from selectively aligned molecules was performed using femtosecond UV laser pulses to excite $C_2F_4I_2$ molecules, and picosecond electron pulses to capture the diffraction patterns [23, 24]. The structural changes triggered by the laser are the same as those shown in figure 3, but improved temporal resolution and a higher fraction of excited molecules made it possible to detect the resulting anisotropy in the diffraction patterns. Figure 6 shows experimental and theoretical diffraction patterns captured at different time delays between the excitation pulse and the electron pulse. A reference pattern taken before the laser excitation ($t < 0$) is subtracted from the diffraction patterns. For delays of less than 5 ps (figures 6(a) and (b)), there is a clear anisotropy in the diffraction pattern. The anisotropy vanishes at later times, and the diffraction patterns recover the circular symmetry (figure 6(c)). The initial degree of alignment was $\langle\cos^2\theta\rangle = 0.5$, and it was found to decay exponentially with a time constant of 2.6 ps after the laser excitation. The expected maximum alignment due to the angular dependence of the photoexcitation is $\langle\cos^2\theta\rangle = 0.6$, but in this case the measurement was limited by the temporal resolution and thus the measured alignment was lower.

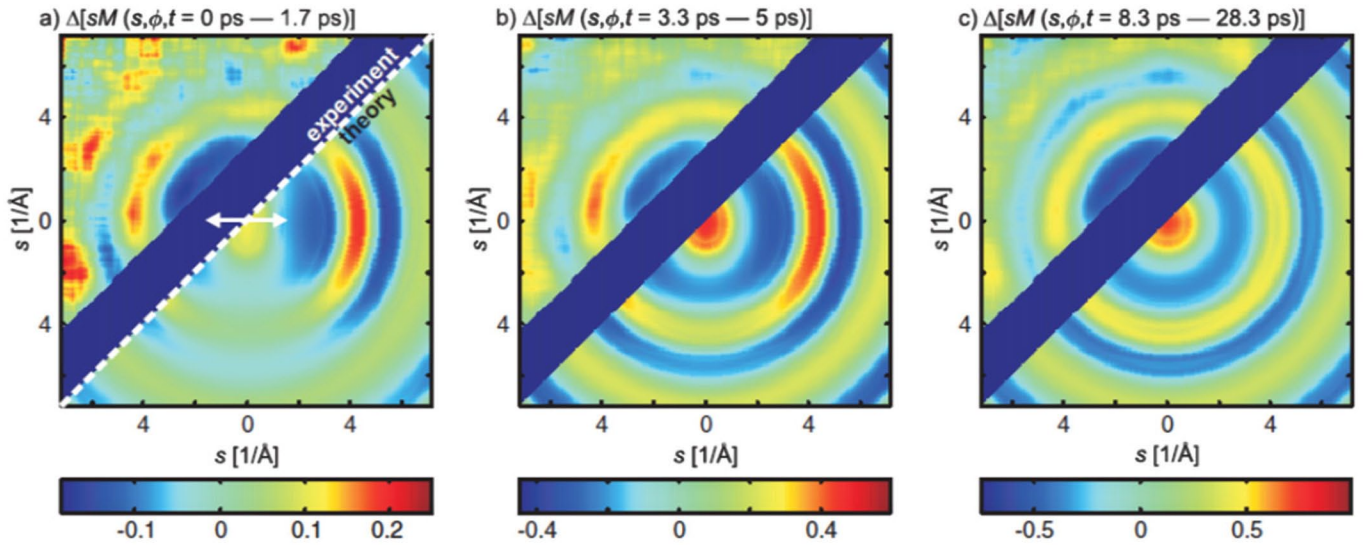

Figure 6. 2D time-resolved difference-diffraction patterns. (**a**) Δ*sM* close to zero time delay. The white arrow indicates the direction of laser polarization. The upper left half of the image displays the experimental data, while the lower right half shows the theoretical prediction. The dark region splitting the image is the shadow of the beam stop. (**b**) Δ*sM* averaged between *t* = 3.3 ps and *t* = 5 ps. (**c**) Δ*sM* averaged between *t* = 8.3 ps and *t* = 28.3 ps. Figure reproduced from [23].

4.4. Imaging of molecules by electron diffraction from impulsively aligned molecules

Diffraction from aligned molecules has the potential for retrieving molecular structures directly from experimental data without the use of a theoretical model of the molecule. This potential, however, was not realized until recently. In order to demonstrate the full potential of diffraction from aligned molecules, two challenges had to be overcome: (i) experimentally, it was necessary to improve the degree of alignment and the signal to noise ratio in the diffraction pattern. (ii) Theoretically, a retrieval method that could be applied to partially aligned molecules was needed. Previous theoretical work had shown that structures could be retrieved for perfectly or very highly aligned molecules [16, 17, 20], while experimentally the alignment that can be achieved is limited.

Impulsive alignment can be improved by decreasing the initial rotational temperature of the molecules and by increasing the intensity of the alignment laser. The laser intensity is limited by multiphoton excitation and ionization events that can distort the molecular structure [25]. For small molecules in the gas phase, multiphoton ionization typically becomes significant at laser intensities around 10^{13} W cm^{-2} [68]. The initial temperature of the molecules can be reduced but only at the expense of reducing the density of the sample. In order to have sufficient scattering, experiments need to reach a compromise between the sample density and initial temperature. Laser alignment experiments that reach a high degree of alignment ($\langle\cos^2\theta\rangle > 0.8$), require an initial rotational temperature on the order of 1 K, which limits the density to approximately 10^8 molecules cm^{-3} [69]. Time-resolved diffraction experiments usually operate at densities on the order of 10^{15}–10^{16} molecules cm^{-3} to achieve adequate signal to noise ratio on the diffraction pattern at sufficiently large scattering angles to reach sub-angstrom resolution. This has so far limited the initial rotational temperature to greater than 20 K. The experimental constraints on the temperature of the molecules and the intensity of the alignment laser pulse has limited the degree of alignment that can be achieved in diffraction experiments to less than $\langle\cos^2\theta\rangle = 0.6$. This alignment is sufficient when dealing with small molecules, but may not be sufficient for larger molecules. The lower density of highly aligned molecules could in principle be partially compensated with the use of high brightness and high repetition rate electrons guns [43, 70], and by the increased contrast in the diffraction pattern of highly aligned molecules [66]. For large molecules such as proteins, adiabatic alignment may provide sufficient alignment for structure retrieval [20, 71].

The first experiments on electron diffraction from impulsively aligned molecules were performed with symmetric top molecules [18]. Trifluoroiodomethane (CF_3I) molecules were aligned by femtosecond laser pulses with a wavelength of 800 nm, and the diffraction patterns were captured with femtosecond electron pulses. The lifetime of the alignment was approximately a picosecond, thus it was critical to reach a resolution below a picosecond. In order to achieve sub-picosecond resolution, the source-to-sample distance was only 10 cm and the charge was kept to 2000 electrons/pulse to reduce space charge broadening. The size of the gas, electron and laser beams was reduced to 100 μm to minimize GVM. This, combined with a high repetition rate (10 kHz) resulted in high quality diffraction patterns with a temporal resolution of 850 fs that was limited mostly by GVD. The use of a supersonic gas jet of molecules seeded in Helium resulted in laser aligned molecules with $\langle\cos^2\theta\rangle = 0.5$.

Even though diffraction patterns with good signal-to-noise ratio (SNR) were captured with this method, the challenge to retrieve the structures remained due to the relatively weak alignment. One key for success was to recognize that while there

may not be sufficient information in a single diffraction pattern, multiple diffraction patterns corresponding to different projections could be recorded by rotating the alignment axis with respect to the electron beam direction. This can be achieved simply by rotating the direction of the laser polarization, in the experimental geometry where laser and electron beams are perpendicular. The next step is to combine the information from the different diffraction patterns to retrieve the ideal diffraction pattern (corresponding to perfectly aligned molecules), on which existing algorithms can be used to retrieve the structure. The main idea here is to first undo the convolution that results from partial alignment and recover the ideal diffraction pattern, and then apply a phase retrieval algorithm on the recovered ideal pattern to retrieve the structure. The first step in this process (the deconvolution) relies on the fact that if the ideal diffraction pattern is known, the diffraction pattern corresponding to any angular distribution can be calculated by a combination of rotation and averaging. Of course, the ideal pattern is not known, but one can use a genetic algorithm to iteratively guess the ideal pattern that, when averaged according to the experimental angular distributions, would produce the measured diffraction patterns. This deconvolution produces only the intensity of the ideal diffraction pattern (not the phase), and requires knowledge of the angular distribution of the molecules, but not the structure.

A genetic algorithm was used to reconstruct the ideal pattern by using three diffraction patterns that corresponded to the alignment axis at 90° to the electron beam, a 60° projection and the pattern with random orientation. The algorithm starts with a random guess for the ideal pattern. From this initial guess, the three patterns are calculated. The calculated patterns are then compared with the measured ones, and an error is defined from the root-mean-square difference between calculated and measured data. A random change is made in the guessed ideal pattern, and the error calculated again. If the error decreases the change is kept, and if the error increases the change is discarded. Whereas the angular distribution can be measured independently [72–76], in this case multiple angular distributions were calculated and the algorithm was used to optimize also for the angular distribution. The algorithm was run with different angular distributions for the aligned patterns, and the one that resulted in the smallest error ($\langle\cos^2\theta\rangle = 0.5$) was kept. After approximately 10^5 iterations, the error no longer decreases, and the algorithm produces a guess for the ideal pattern. Figure 7(a) shows the ideal pattern from theory and (b) shows the pattern retrieved from the experimental data using the genetic algorithm. The main features of the theoretical pattern are reproduced in the experimental pattern, although there are some minor differences. The true test of the method is to retrieve the structure. Once this ideal pattern was generated, the holographic retrieval method [17] was used to retrieve the structure in cylindrical coordinates. The holographic method requires that the molecule contain one heavy atom that scatters more strongly than the rest, in this case the iodine atom. Figures 7(c) and (d) show the structures retrieved from the ideal theoretical and experimental patterns, respectively.

Figure 7(d) is the first demonstration of the retrieval of atomically resolved images of isolated molecules directly from experimental data. The white dots show the theoretical positions of the atoms. The structures are resolved in two cylindrical coordinates (r and z). In this reconstruction the three F atoms overlap at the same position. The cylindrical reconstruction is due to the simplified structure retrieval method used for this demonstration, and not a limitation due to 1D alignment. The method clearly reaches atomic resolution, and the atomic position and the main molecular angle are retrieved with an accuracy better than 10%. Further theoretical analysis revealed that the limiting factors to the accuracy of the retrieval were the degree of alignment and the range of scattering angles that were captured. Both of these limitations can be improved by using brighter electrons sources that will result in more scattering and allow for working with lower density (colder) samples and thus higher alignment.

5. Recent advances and limitations of molecular imaging with electron pulses

5.1. Structure retrieval and improved alignment

Recent theoretical work has shown that structures can also be retrieved in 3D, beyond the cylindrical projections demonstrated experimentally, and for more complex molecules [19]. Figure 8 shows the structure of the trifluorotoluene ($C_6H_5CF_3$) molecules retrieved from simulated diffraction patterns. The green regions in the figure indicate the retrieved positions of the nuclei, in good agreement with the known structure. In this work a two-step retrieval method was used. First, a genetic algorithm was used to calculate the ideal diffraction pattern (corresponding to $\langle\cos^2\theta\rangle = 1$) starting from two patterns: one with partial alignment ($\langle\cos^2\theta\rangle = 0.56$) and one with randomly oriented molecules. The structure was retrieved from the ideal pattern using an iterative algorithm that splits the diffraction pattern into cylindrical harmonics [16, 20]. Each harmonic is Fourier transformed between the diffraction and the object plane. Constraints are applied at the object plane iteratively, and in the diffraction plane the retrieved phase is combined with the measured amplitude. The algorithm used an atomicity constraint that forces the structure to be composed of individual atoms (as opposed to a continuous structure). This constraint is important in achieving a correct structure, and can only be applied if the method has sub-Angstrom resolution. The patterns were simulated to $s_{Max} = 19$ Å^{-1}, about 2.5 times larger coverage than previous experiments, which would require about 20 times more scattered electrons to be detected.

The accuracy of the retrieval method increases with the degree of alignment. Impulsive alignment can be improved by using a sequence of laser pulses [77], but is ultimately limited by the initial rotational temperature of the molecules and the maximum intensity that can be applied. Recent UED experiments have shown that impulsive alignment reaches a saturation value for intensities well below the ionization threshold, and that at

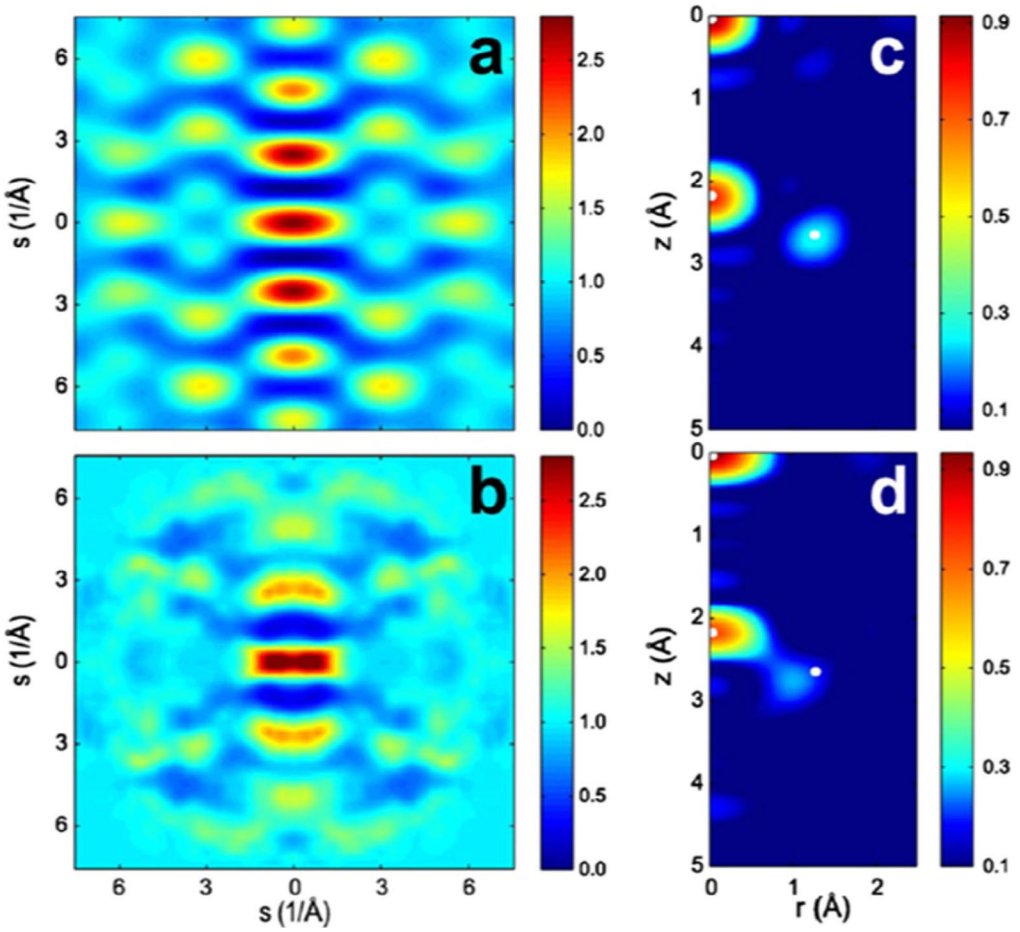

Figure 7. Molecular structure retrieved from diffraction patterns for the CF_3I molecule. (**a**), (**c**) Theoretical diffraction pattern (sM/s) for perfectly aligned molecules and the corresponding molecular image. (**b**), (**d**) Experimentally retrieved pattern for perfectly aligned molecules and the corresponding molecular image. The white dots in panels (c) and (d) indicate the expected position of each atom. Figure reproduced from [18].

high intensities the structure can be distorted by multiphoton excitation [25]. Another option to improve the alignment is a mixed alignment with shaped laser pulses to do adiabatic turn-on and impulsive turn-off of the alignment field [78, 79]. In this method, the laser pulse has a long leading edge of nanosecond duration and a very fast (femtosecond) drop off after the peak intensity. The molecules are aligned adiabatically and since the laser intensity turns off in a time much shorter than the rotational time, they remain aligned for a short time in a field free environment. This method, however, is challenging to implement because it requires a laser pulse with a large spectral bandwidth to support the femtosecond turn off and also high pulse energy to reach a high intensity during the turn on. Such laser parameters are not available in most laboratories, and can typically only be achieved at low repetition rates that are not suitable for UED experiments where high count rates are needed.

Improved field-free alignment could be achieved by combining impulsive alignment (or mixed) and selection. In this method, the molecules would first be aligned impulsively by a

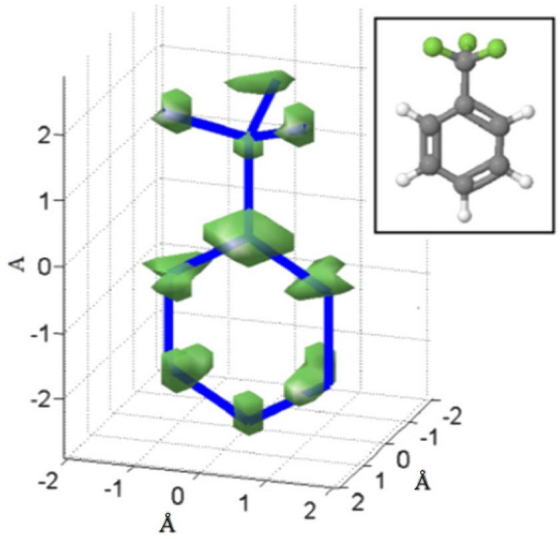

Figure 8. 3D structure retrieved from simulated diffraction patterns. Isosurface rendering of the reconstructed 3D molecular structure of trifluorotoluene. The overlapped blue sticks show the frame of the molecules with non-hydrogen atoms in both ends of each stick. The ball and stick model of the molecules is shown in the inset. This form should not be understood as alternating single and double bonds in the ring but as one continuous bond. Figure reproduced from [19].

non-resonant laser pulse. The delay between excitation and the peak alignment is a few picoseconds, depending on the laser parameters and the moment of inertia of the molecule. When the distribution is near the peak alignment, a second resonant excitation pulse is used to trigger a photochemical reaction. The total anisotropy will be higher than with each method on its own. The timescale for atomic motion is typically hundreds of femtoseconds, while impulsive alignment in small molecules survives for one or a few picoseconds. If the temporal resolution of the probing electron diffraction is sufficiently fast, the structures of the transient states can in principle be determined in 3D, provided the dynamics are significantly faster than the lifetime of the alignment. For dynamics on longer time scales, the structure retrieval will be complicated by a changing angular distribution and will require deconvolution.

5.2. Temporal resolution

The two main limitations for improving the temporal resolution in gas phase UED are delivering short electron pulses on the target and minimizing GVM between electrons and laser as they traverse the sample. Two approaches are currently being pursued to improve resolution. The first is to use an RF cavity to compress electron pulses at the target [42, 43] and to use a laser pulse with a tilted wavefront to match the velocity of the electrons [46]. The RF cavity has a time-dependent longitudinal electric field that accelerates the back of the electron pulse and slows down the leading edge, such that the pulse will self-compress and reach a minimum pulse duration at the position of the sample. A pulse duration of about 200 fs FWHM has been demonstrated, but temporal jitter has limited the achievable resolution to between 300 and 400 fs [13, 80, 81]. An important advantage of using an RF cavity (compared to a compact gun with only DC fields) is that the sample can be placed at a larger distance from the source, while increasing the number of electron per pulse and keeping the same pulse duration. With a gas phase sample it would be technically challenging to have a gas jet very close to the photocathode, because in order to deliver short electron pulses, the extraction electric field on the photocathode must be very large, which requires a high vacuum. The higher current of the electron beam will correspondingly increase the number of scattered electrons, and thus improve the spatial resolution as well by improving the SNR, in particular for the larger scattering angles. The main limitation of the RF guns is the timing jitter, but this can in principle be corrected using time-stamping [38]. However, the use of RF compression can result in reduced coherence.

There is a trade-off between number of electrons, coherence, pulse duration and beam size. Ultimately the performance can be improved by having a source with higher brightness, and sacrificing charge to improve other parameters. The GVM can be compensated by bringing the laser pulse at an angle with respect to the electron pulse, and tilting the laser pulse-front such that it is parallel to the pulse front of the electron beam. In this way the velocity component of the laser in the direction parallel to the electrons can be matched to the electron velocity as the pulses traverse the sample. The dispersion used for pulse tilting means that the laser pulse can only be fully compressed in time at one plane and will be broadened before and after that plane. It has been recently demonstrated that the velocity of a 100 keV electron pulse can be matched over a length of 1 mm while keeping the laser pulse duration below 100 fs [46]. This length is sufficient for a gas target. Combining RF compression with pulse tilting, it is expected that the temporal resolution of gas-phase UED experiments will be limited by the jitter between laser and electron pulses. It has been demonstrated that the RF timing error can be suppressed to below 100 fs [53], which could potentially lead to a ~100 fs time-of-arrival jitter between laser and electron beam. In addition, the jitter could potentially be solved using time-stamping techniques, similar to those developed for x-ray free electron lasers [82, 83] or for condensed matter UED [38].

The second approach is to use relativistic electron pulses, with energies in the range of 1–5 MeV, which can be generated using an RF photoelectron gun [47–53]. A laser pulse is used to trigger the photoemission while an accelerating RF field is present. The high electron kinetic energy can make GVM negligible. For example, the group velocity for an electron pulse of 3.7 MeV kinetic energy is $v = 0.993c$. This results in a 20 fs delay with respect to an optical pulse per millimeter of interaction length, while gas beams can be made significantly smaller than a millimeter. Another advantage of MeV electrons is that the effect of space charge is greatly diminished for relativistic electrons, so that pulse broadening is less severe. The main limitation in the resolution for pump-probe experiments will be the temporal drifts and jitter between the electrons and laser. Recent progress in MeV electron experiments and synchronization shows that sub-200 fs resolution is within reach [53, 84]. The main disadvantage of MeV electron guns is that they are more costly than the more compact keV electron guns, and require significant radiation shielding.

There has also been recent progress on alternative methods to determine the structure of gas phase molecules with femtosecond resolution. One method to improve the temporal resolution is laser-induced electron diffraction, where a high intensity femtosecond laser pulse ionizes the molecule (removing an electron) and then accelerates the electron back towards the ionized molecule [85–87]. The advantage of this method it that it can in principle reach a resolution of a few femtoseconds, while the disadvantage is that the molecules are immersed in a strong laser field while they are being probed, which might alter the path of a reaction. This method has so far only been applied to linear molecules, but research is ongoing to apply it to more complex molecules [88]. In a different approach that was recently demonstrated, the velocity mismatch and temporal resolution problems in gas phase diffraction were solved by using femtosecond x-ray pulses from a free-electron laser, but the experiment could not reach atomic resolution in space due to the much weaker scattering of x-rays compared to electrons. [89].

6. Outlook

The ultimate goal of gas-phase UED, to capture the position of all nuclei during a molecular reaction, requires further improvements in the average current of electron sources and the temporal resolution. A significant improvement would be to use MeV RF guns at higher repetition rates, which can in principle operate at MHz repetition rates [70]. This would require ultrafast lasers with high average power to perform pump-probe experiments at high repetition rates. An RF cavity can also be used to compress MeV electrons, resulting in shorter pulses and more charge per pulse [90], improving both the beam current and temporal resolution. While RF compression for keV electron pulses has not yet been used for gas-phase UED, compression cavities can currently operate at rates of tens of kilohertz and significantly reduce the pulse duration and increase the charge of the bunches. All of these compression methods come at the expense of a timing jitter between laser and electrons. The ultimate solution could be to tag the time of arrival of each electron pulse with respect to the laser, using a streak camera [38, 91], an RF cavity with a transverse field [92] or an ultrafast process with a known temporal evolution that is measured simultaneously with the diffraction pattern.

With these improvements, UED is well positioned to investigate ultrafast reactions in small molecules. Further developments, in particular brighter electron sources, will be needed to target large molecules where a large transverse coherence and high beam charge will be needed. Capturing the 3D structure of larger molecules will require aligning them, which has not yet been extensively investigated, and delivering the sample molecules in a beam. Several methods have been developed to deliver large molecules for x-ray diffraction experiments at free-electron lasers [93], which could also be applied for electron diffraction. Additional improvements are also needed in the structure retrieval methods. Whereas there are several methods to retrieve structure from perfectly aligned molecules, and a two-step method was found to be successful in retrieving structures from partially aligned molecules, these methods still need to be tried on a case-by-case basis for different molecules. A more general method that could be used for any molecular geometry would be extremely valuable, in the same way that it was important for the GED community to develop standard tools for structure retrieval.

In summary, gas-phase UED has already proven a successful method to investigate transient molecular structures with picosecond resolution. Diffraction from aligned molecules has added the capability to determine 3D molecular structures directly from the data without the need of a theoretical model. Ultimately, a resolution below 100 fs and increased beam current will be needed to observe the fastest processes in more complex molecules. Judging by recent and ongoing progress, this goal seems feasible within the next few years.

Acknowledgments — This work was supported by the US Department of Energy Office of Science, Office of Basic Energy Sciences under Award Number DE-SC0003931.

References

[1] Pedersen S, Herek J L and Zewail A H 1994 The validity of the 'diradical' hypothesis: direct femtosecond studies of the transition-state structures *Science* 266 1359

[2] Waldeck D H 1993 Photoisomerization dynamics of stilbenes in polar solvents *J. Mol. Liq.* 57 127–48

[3] Schoenlein R W, Peteanu L A, Mathies R A and Shank C V 1991 The first step in vision: femtosecond isomerization of rhodopsin *Science* 254 412

[4] Mathies R A, Brito Cruz C H, Pollard W T and Shank C V 1988 Direct observation of the femtosecond excited-state cis-trans isomerization in bacteriorhodopsin *Science* 240 777

[5] Weiss S 1999 Fluorescence spectroscopy of single biomolecules *Science* 283 1676

[6] Milne C J, Penfold T J and Chergui M 2014 Recent experimental and theoretical developments in time-resolved x-ray spectroscopies *Coord. Chem. Rev.* 277 44–68

[7] Sil S and Umapathy S 2014 Raman spectroscopy explores molecular structural signatures of hidden materials in depth: universal multiple angle Raman spectroscopy *Sci. Rep.* 4 5308

[8] Blanchet V, Zgierski M Z, Seideman T and Stolow A 1999 Discerning vibronic molecular dynamics using time-resolved photoelectron spectroscopy *Nature* 401 52–4

[9] Bisgaard C Z, Clarkin O J, Wu G, Lee A M D, Gebner O, Hayden C and Stolow A 2009 Time-resolved molecular frame dynamics of fixed-in-space CS2 molecules *Science* 323 1464

[10] Gessner O *et al* 2006 Femtosecond multidimensional imaging of a molecular dissociation *Science* 311 219

[11] Deb S and Weber P M 2011 The ultrafast pathway of photon-induced electrocyclic ring-opening reactions: the case of 1,3- cyclohexadiene *Annu. Rev. Phys. Chem.* 62 19–39

[12] Henderson R 1995 The potential and limitations of neutrons, electrons and x-rays for atomic resolution microscopy of unstained biological molecules *Q. Rev. Biophys.* 28 171

[13] Gao M *et al* 2013 Mapping molecular motions leading to charge delocalization with ultrabright electrons *Nature* 496 343–6

[14] Miller R J D 2014 Mapping atomic motions with ultrabright electrons: the chemists' Gedanken experiment enters the lab frame *Ann. Rev. Phys Chem.* 65 583–604

[15] Hargittai I and Hargittai M 1988 *Stereochemical Applications of Gas-Phase Electron Diffraction* (New York: VCH)

[16] Saldin D K, Shneerson V L, Starodub D and Spence J C H 2010 Reconstruction from a single diffraction pattern of azimuthally projected electron density of molecules aligned parallel to a single axis *Acta Cryst.* A 66 32–7

[17] Ho P J, Starodub D, Saldin D K, Shneerson V L, Ourmazd A and Santra R 2009 Molecular structure determination from x-ray scattering patterns of laser-aligned symmetric-top molecules *J. Chem. Phys.* 131 131101

[18] Hensley C J, Yang J and Centurion M 2012 Imaging of isolated molecules with ultrafast electron pulses *Phys. Rev. Lett.* 109 133202

[19] Yang J, Makhija V, Kumarappan V and Centurion M 2014 Reconstruction of three-dimensional molecular structure from diffraction of laser-aligned molecules *Struct. Dyn.* 1 044101

[20] Spence J C H, Schmidt K, Wu J S, Hembree G, Weierstall U, Doak B and Fromme P 2005 Diffraction and imaging from a beam of laser-aligned proteins: resolution limits *Acta Cryst.* A 61 237–45

[21] Volkmer M, Meier C, Mihill A, Fink M and Böwering N 1992 Elastic electron scattering from CH3I molecules oriented in the gas phase *Phys. Rev. Lett.* 68 2289

[22] Hoshina K, Yamanouchi K, Ohshima T, Ose Y and Todokoro H 2003 Alignment of CS2 in intense nanosecond laser fields probed by pulsed gas electron diffraction *J. Chem. Phys.* 118 6211

[23] Reckenthaeler P R, Centurion M, Fuss W, Trushin S A, Krausz F and Fill E 2009 Time-resolved electron diffraction from selectively aligned molecules *Phys. Rev. Lett.* 102 213001

[24] Centurion M, Reckenthaeler P, Krausz F and Fill E 2010 Picosecond electron diffraction from molecules aligned by dissociation *J. Mol. Struct.* 978 141–6

[25] Yang J, Beck J, Uiterwaal C J and Centurion M 2015 Imaging of alignment and structural changes of carbon disulfide molecules using ultrafast electron diffraction *Nat. Commun.* 6 8172

[26] Mark H and Wierl R 1930 Über Elektronenbeugung am einzelnen molekül *Naturwissenschaften* 18 205

[27] Sim G A, Sutton L E, Bartell L S, Romenesko D J and Wong T C 1975 *Molecular Structure by Diffraction Methods* vol 3 (London: The Chemical Society) pp 78–80

[28] Blom R, Cradock S, Davidson S L and Rankin D W H 1991 The molecular structure of 1,3,5-trichlorobenzene determined by combined analysis of gas-phase electron diffraction and liquid crystal NMR data *J. Mol. Struct.* 245 369–77

[29] Davis M J, Rankin D W H and Cradock S 1990 The gas-phase structure of PF2OCH3, determined by combined analysis of electron diffraction and rotational data *J. Mol. Struct.* 238 273–87

[30] Klimkowski V, Ewbank J D, Van Alsenoy C, Scarsdale J N and Schäfer L 1982 Molecular orbital constrained electron diffraction studies: IV. Conformational analysis of the methyl ester of glycine *J. Am. Chem. Soc.* 104 1476–80

[31] Mitzel N W and Rankin D W H 2003 Molecular structures from theory and experiment: the best of both worlds *Dalton Trans.* 19 3650–62

[32] Prince E 2004 *International Tables for Crystallography Volume C: Mathematical, Physical and Chemical Tables* (New York: Springer)

[33] Siwick B J, Dwyer J R, Jordan R E and Miller R J D 2003 An atomic-level view of melting using femtosecond electron diffraction *Science* 302 1382

[34] Sciaini G and Miller R J D 2011 Femtosecond electron diffraction: heralding the era of atomically resolved dynamics *Reports Prog. Phys.* 74 096101

[35] Gerbig C, Senftleben A, Morgenstern S, Sarpe C and Baumert T 2015 Spatio-temporal resolution studies on a highly compact ultrafast electron diffractometer *New J. Phys.* 17 043050

[36] Williamson J C and Zewail A H 1993 Ultrafast electron diffraction, velocity mismatch and temporal resolution in crossed-beam experiments *Chem. Phys. Lett.* 209 10–6

[37] Siwick B J, Dwyer J R, Jordan R E and Miller R J D 2002 Ultrafast electron optics: propagation dynamics of femtosecond electron packets *J. Appl. Phys.* 92 1643–8

[38] Gao M, Jiang Y, Kassier G H and Miller R J D 2013 Single shot time stamping of ultrabright radio frequency compressed electron pulses *Appl. Phys. Lett.* 103 033503

[39] Sciaini G *et al* 2009 Electronic acceleration of atomic motions and disordering in bismuth *Nature* 458 56–9

[40] Geiser J D and Weber P M 1995 High-repetition-rate time-resolved gas phase electron diffraction *Proc. SPIE* 2521 136–44

[41] Lahme S, Kealhofer C, Krausz F and Baum P 2014 Femtosecond single-electron diffraction *Struct. Dyn.* 1 034303

[42] van Oudheusden T, de Jong E F, van der Geer S B, Op 't Root W P E M, Luiten O J and Siwick B J 2007 Electron source concept for single-shot sub-100 fs electron diffraction in the 100 keV range *J. Appl. Phys.* 102 093501

[43] van Oudheusden T, Pasmans P L E M, van der Geer S B, de Loos M J, van der Wiel M J and Luiten O J 2010 Compression of subrelativistic space-charge-dominated electron bunches for single-shot femtosecond electron diffraction *Phys. Rev. Lett.* 105 264801

[44] Danielius R, Piskarskas A, Di Trapani P, Andreoni A, Solcia C and Foggi P 1996 Matching of group velocities by spatial walk-off in collinear three-wave interaction with tilted pulses *Opt. Lett.* 21 973–5

[45] Baum P and Zewail A H 2006 Breaking resolution limits in ultrafast electron diffraction and microscopy *PNAS* 134 16105

[46] Zhang P, Yang J and Centurion M 2014 Tilted femtosecond pulses for velocity matching in gas-phase ultrafast electron diffraction *New J. Phys.* 16 083008

[47] Hastings J B, Rudakov F M, Dowell D H, Schmerge J F, Cardoza J D, Castro J M, Gierman S M, Loos H and Weber P M 2006 Ultrafast time-resolved electron diffraction with megavolt electron beams *Appl. Phys. Lett.* 89 184109

[48] Li R, Tang C, Du Y, Huang W, Du Q, Shi J, Yan L and Wang X 2009 Experimental demonstration of high quality MeV ultrafast electron diffraction *Rev. Sci. Instrum.* 80 083303

[49] Zhu P *et al* 2015 Femtosecond time-resolved MeV electron diffraction *New J. Phys.* 17 063004

[50] Wang X, Qiu X and Ben-Zvi I 1996 Experimental observation of high-brightness microbunching in a photocathode rf electron gun *Phys. Rev.* E 54 R3121–4

[51] Wang X J, Wu Z and Ihee H 2003 Femto-seconds electron beam diffraction using photocathode RF gun *Proc. Part. Accel. Conf.* 1 420–2

[52] Manz S *et al* 2015 Mapping atomic motions with ultrabright electrons: towards fundamental limits in space-time resolution *Faraday Discuss.* 177 467–91

[53] Weathersby S P *et al* 2015 Mega-electron-volt ultrafast electron diffraction at SLAC national accelerator laboratory *Rev. Sci. Instrum.* 86 073702

[54] Ischenko A A, Golubkov V V, Spridonov V P, Zgurskii A V, Akhmanov A S and Vabischevich M G 1983 A stroboscopical gas-electron diffraction method for the investigation of short-lived molecular species *Appl. Phys.* B 32 161

[55] Ewbank J D, Luo J Y, English J T, Liu R, Faust W L and Schaefer L 1993 Time-resolved gas electron diffraction study of the 193 nm photolysis of 1,2-dichloroethenes *J. Phys. Chem.* 97 8745

[56] Williamson J C, Cao J, Ihee H, Frey H and Zewail A 1997 Clocking transient chemical changes by ultrafast electron diffraction *Nature* 386 159

[57] Ihee H, Lobastov V A, Gomez U M, Goodson B M, Srinivasan

R, Ruan C Y and Zewail A H 2001 Direct imaging of transient molecular structures with ultrafast diffraction *Science* 291 458

[58] Dudek R C and Weber P M 2001 Ultrafast diffraction imaging of the electrocyclic ring-opening reaction of 1,3- cyclohexadiene *J. Phys. Chem.* A 105 4167–71

[59] Zhong D, Ahmad S and Zewail A H 1997 Femtosecond elimination reaction dynamics *J. Am. Chem. Soc.* 119 5978–9

[60] Stapelfeldt H and Seideman T 2003 Colloquium: aligning molecules with strong laser pulses *Rev. Mod. Phys.* 75 543

[61] Ortigoso J, Rodriguez M, Gupta M and Friedrich B 1999 Time evolution of pendular states created by the interaction of molecular polarizability with a pulsed nonresonant laser field *J. Chem. Phys.* 110 3870–5

[62] Seideman T and Hamilton E 2005 Nonadiabatic alignment by intense pulses, concepts, theory, and directions *Adv. At. Mol. Opt. Phys.* 52 289–329

[63] Bijwering N, Volkmer M, Meier C, Lieschke J and Dreier R 1995 Electron diffraction from oriented molecules and implications for molecular structure analysis *J. Mol. Struct.* 348 49–52

[64] Williamson J C and Zewail A H 1994 Ultrafast electron diffraction: IV. Molecular structures and coherent dynamics *J. Phys. Chem.* 98 2766

[65] Baskin J S and Zewail A H 2005 Ultrafast electron diffraction: oriented molecular structures in space and time *Chem. Phys. Chem.* 6 2261

[66] Yang J and Centurion M 2015 Gas phase electron diffraction from laser-aligned molecules *Struct. Chem.* 26 1513–20

[67] Saldin D K *et al* 2010 Structure of a single particle from scattering by many particles randomly oriented about an axis: toward structure solution without crystallization? *New J. Phys.* 12 035014

[68] Scarborough T D, Strohaber J, Foote D B, McAcy C J and Uiterwaal C J G J 2011 Ultrafast REMPI in benzene and the monohalobenzenes without the focal volume effect *Phys. Chem. Chem. Phys.* 13 13783–90

[69] Trippel S, Mullins T, Mueller N, Kienitz J S, Długolecki K and Küpper J 2013 Strongly aligned and oriented molecular samples at a kHz repetition rate *J. Mol. Phys.* 111 1738–43

[70] Sannibale F, Filippetto D and Papadopoulos C F 2011 Schemes and challenges for electron injectors operating in high repetition rate x-ray FELs *J. Mod. Opt.* 58 1419–37

[71] Starodub D *et al* 2005 Damped and thermal motion of laser-aligned hydrated macromolecule beams for diffraction *J. Chem. Phys.* 123 244304

[72] Chen Y-H, Varma S and Milchberg H M 2008 Space- and time-resolved measurement of rotational wave packet revivals of linear gas molecules using single-shot supercontinuum spectral interferometry *J. Opt. Soc. Am.* B 25 B122–32

[73] Litvinyuk I V, Lee K F, Dooley P W, Rayner D M, Villeneuve D M and Corkum P B 2003 Alignment-dependent strong field ionization of molecules *Phys. Rev. Lett.* 90 233003

[74] Itatani J, Zeidler D, Levesque J, Spanner M, Villeneuve D M and Corkum P B 2005 Controlling high harmonic generation with molecular wave packets *Phys. Rev. Lett.* 94 123902

[75] McFarland B K, Farrell J P, Bucksbaum P H and Guhr M 2008 High harmonic generation from multiple orbitals in N2 *Science* 322 1232

[76] Ren X, Makhija V and Kumarappan V 2012 Measurement of field-free alignment of jet-cooled molecules by nonresonant femtosecond degenerate four-wave mixing *Phys. Rev.* A 85 033405

[77] Cryan J P, Bucksbaum P H and Coffee R N 2009 Field-free alignment in repetitively kicked nitrogen gas *Phys. Rev.* A 80 063412

[78] Seideman T 2001 On the dynamics of rotationally broad, spatially aligned wave packets *J. Chem. Phys.* 115 5965

[79] Sussman B J, Underwood J G, Lausten R, Ivanov M Y and Stolow A 2006 Quantum control via the dynamic Stark effect: application to switched rotational wave packets and molecular axis alignment *Phys. Rev.* A 73 053403

[80] Chatelain R P, Morrison V R, Godbout C and Siwick B J 2012 Ultrafast electron diffraction with radio-frequency compressed electron pulses *Appl. Phys. Lett.* 101 081901

[81] Mancini G F, Mansart B, Pagano S, van der Geer B, de Loos M and Carbone F 2012 Design and implementation of a flexible beamline for fs electron diffraction experiments *Nucl. Instrum. Methods Phys. Res. A* 691 113–22

[82] Beye M *et al* 2012 X-ray pulse preserving single-shot optical cross-correlation method for improved experimental temporal resolution *Appl. Phys. Lett.* 100 1–5

[83] Harmand M *et al* 2013 Achieving few-femtosecond time-sorting at hard x-ray free-electron lasers *Nat. Photon.* 7 215–8

[84] Murooka Y, Naruse N, Sakakihara S, Ishimaru, Yang M J and Tanimura K 2011 Transmission-electron diffraction by MeV electron pulses *Appl. Phys. Lett.* 98 251903

[85] Zuo T, Bandrauk A D and Corkum P B 1996 Laser-induced electron diffraction: a new tool for probing ultrafast molecular dynamics *Chem. Phys. Lett.* 259 313–20

[86] Blaga C I *et al* 2012 Imaging ultrafast molecular dynamics with laser-induced electron diffraction *Nature* 483 194–7

[87] Pullen M G *et al* 2015 Imaging an aligned polyatomic molecule with laser-induced electron diffraction *Nat. Commun.* 6 7262

[88] Yu C, Wei H, Wang X, Le A T, Lu R and Lin C D 2015 Reconstruction of two-dimensional molecular structure with laser-induced electron diffraction from laser-aligned polyatomic molecules *Sci. Rep.* 5 15753

[89] Minitti M P *et al* 2015 Imaging molecular motion: femtosecond x-ray scattering of an electrocyclic chemical reaction *Phys. Rev. Lett.* 114 255501

[90] Lu X H, Tang C X, Li R K, To H, Andonian G and Musumeci P 2015 Generation and measurement of velocity bunched ultrashort bunch of pC charge *Phys. Rev. ST Accel. Beams* 18 032802

[91] Kassier G H, Haupt K, Erasmus N, Rohwer E G, von Bergmann H M, Schwoerer H, Coelho S M M and Auret F D 2010 A compact streak camera for 150 fs time resolved measurement of bright pulses in ultrafast electron diffraction *Rev. Sci. Instrum.* 81 105103

[92] Scoby C M, Li R K, Threlkeld E, To H and Musumeci P 2013 Single-shot 35 fs temporal resolution electron shadowgraphy *Appl. Phys. Lett.* 102 023506

[93] Spence J C H, Weierstall U and Chapman H N 2012 X-ray lasers for structural and dynamic biology *Rep. Prog. Phys.* 75 102601